Title: Cell size and wall dimensions drive distinct variability of earlywood and latewood density in Northern Hemisphere conifers

Brief heading: Cell dimensions drive distinct variability in earlywood and latewood density

Authors: Jesper Björklund[1], Kristina Seftigen[1, 2, 3], Fritz Schweingruber[1], Patrick Fonti[1], Georg von Arx[1, 4], Marina V. Bryukhanova[5, 6], Henri E. Cuny[1], Marco Carrer[7], Daniele Castagneri[7] and David C. Frank[1, 8]

Affiliations: [1]Swiss Federal Research Institute for Forest Snow and Landscape (WSL), Zuercherstrasse 111, 8903 Birmensdorf, Switzerland

[2]Gothenburg University Laboratory for Dendrochronology, Department of Earth Sciences, University of Gothenburg, Guldhedsgatan 5a, 40530 Göteborg, Sweden

[3]Université catholique de Louvain, Earth and Life Institute, Georges Lemaître Centre for Earth and Climate Research, Place Louis Pasteur, B-1348 Louvain-la-Neuve, Belgium

[4]Climatic Change and Climate Impacts, Institute for Environmental Sciences, 66 Bvd Carl Vogt, CH-1205 Geneva, Switzerland

[5]V.N. Sukachev Institute of Forest SB RAS, Akademgorodok 50, bld.28, 660036 Krasnoyarsk, Russia

[6]Siberian Federal University, Svobodny pr. 79, 660041 Krasnoyarsk, Russia

[7]University of Padova, Dept. TeSAF, Via dell'Università 16, I-35020 Legnaro (PD), Italy

[8]Laboratory of Tree-Ring Research, University of Arizona, 1215 E Lowell St, Tucson, AZ 85721, USA

Author for correspondence: Jesper Björklund, Swiss Federal Research Institute for Forest Snow and Landscape (WSL), Zuercherstrasse 111, 8903 Birmensdorf, Switzerland. Email: jesper.bjoerklund@wsl.ch Tel: +41 44 739 2816

Total word count:	5596	No. of figures:	8, all in colors
Summary:	200	No. of Tables:	0
Introduction:	1142	No. of Supporting Information files:	1, including 1 table, 9 figures, and 5 Notes
Materials and Methods:	1089		
Results:	1356		
Discussion:	1897		
Acknowledgements:	113		

The following Supporting Information is available for this article:

Tab. S1 Top 10 most common species in the Northern Hemisphere densitometric network.

Fig. S1 X-ray images for ten of the most abundant species in the network

Fig. S2 Map of lengths of chronologies in the NH Network.

Fig. S3 *Rbar* statistic for each chronology and parameter in the NH-network

Fig. S4 Examples how to calculate bivariate univariate density parameters

Fig. S5 Correlation coefficients between different pairs of ring widths, and densities

Fig. S6 Hovmöller diagrams over precipitation correlations of NH-network data

Fig. S7 Complete results of the cluster identification of the NH-network data.

Fig. S8 Standard deviations and averages of different anatomical parameters,

Fig. S9 Correlation coefficients between different anatomical parameters

Notes S1 NH-network quality screening

Notes S2 NH-network overview

Notes S3 Rbar, the strength of the common signal in the NH-network

Notes S4 Cell anatomical data details

Notes S5 List of abbreviations

Summary

- Inter-annual variability of wood density – an important plant functional trait and environmental proxy – in conifers is poorly understood. Therefore we explore the anatomical basis of density. We hypothesize that earlywood density is determined by tracheid size and latewood density by wall dimensions, reflecting their different functional tasks.

- To determine general patterns of variability, density parameters from 27 species and 349 sites across the Northern Hemisphere were correlated to tree-ring width parameters and local climate. We performed the same analyses with density and width derived from anatomical data comprising 2 species and 8 sites. The contributions of tracheid size and wall dimensions to density were disentangled with sensitivity analyses.

- Notably, correlations between density and width shifted from negative to positive moving from earlywood to latewood. Temperature responses of density varied intra-seasonally in strength and sign. The sensitivity analyses revealed tracheid size as the main determinant of earlywood density while wall dimensions become more influential for latewood density.

- Our novel approach of integrating detailed anatomy data with large-scale tree-ring data allowed us to contribute to an improved understanding of inter-annual variations of conifer growth and illustrate how conifers balance investments to the competing xylem functions of hydraulics and mechanical support.

Keywords: Tracheid anatomy, Tree-ring network, Xylem function, Wood density, Ring width, Dendroclimatology

Introduction

Quantifying the spatial and temporal variability of woody tissue in trees is a long-standing research priority (e.g. Fritts, 1976; Hanewinkel et al., 2013; Frank et al., 2015). Considerable efforts during the last decades have led to the assembly of global datasets of annually resolved tree-ring parameters (http://www.ncdc.noaa.gov/paleo), and have foremost been used to set the current climate into a longer-term perspective (e.g. Frank et al., 2010). Similarly, intensive studies of wood anatomical features have been critical to establish general concepts of xylogenesis as well as the structural properties and functional priorities of the xylem (e.g. Tyree & Ewers, 1991; Rossi et al., 2012; Cuny et al., 2014). However, the relatively new approach of measuring *inter-annual* records of anatomical properties (e.g. Bryukhanova and Fonti, 2013; Castagneri et al., 2015; Pritzkow et al., 2013) has not yet reached its full potential, mainly because of technical difficulties in producing data. In the broader context of tree-growth, one of these potentials is to study the link between, on the one hand, widespread and well-replicated tree-ring data (ring width and density), and on the other, the fewer and low-replicated datasets of quantitative wood anatomy (e.g. cell lumen and cell wall). The joint use of tree-ring and anatomical data can have synergetic potential because (1) it may offer a break-through in identifying how the anatomy defines inter-annual variations in density, and in turn facilitate interpretations of how radial growth and wood density are interconnected and climatically controlled. (2) Insights of the anatomical basis of wood density can conversely make wood density a valuable tool for assessing inter-annual variability in xylem architecture and associated functional properties.

The xylem of conifers is essentially composed of tracheid cells that – depending on their anatomical characteristics – are mainly optimized for a) efficient water transport, or b) providing structural support (Tyree & Zimmermann, 2002; Wodzicki, 1971). Early in the growing season cell division is fast and the subsequent cell enlargement occurs for a relatively long time (Cuny et al., 2014). The wall-thickening phase is relatively short but the wall-thickness must be sufficient to minimize the risk of cell implosion causing hydraulic failure (Hacke et al., 2001; Pratt et al., 2007). The resulting tracheids become large (earlywood cells) and supply the bulk of the crowns' water demand. Later in the growing season, cell division slows down, the enlargement phase shortens and the wall-thickening phase extends (Cuny et al., 2014). The

narrower band of thick-walled small-diameter tracheids (latewood cells) works as armature for the tree structure (Larson, 1994), but has limited water transport-capacity due to the narrow tracheid lumina (Sperry et al., 2006). This intra-annual dichotomy balances investments in either earlywood or latewood tissue and represents the continuous attempt to best allocate the available resources to guarantee an adequate and sustainable functioning of the xylem (Sass-Klaassen et al., 2016). In fact, there seems to be considerable *inter-annual* variability in anatomical properties in both earlywood and latewood components (e.g. Bryukhanova and Fonti, 2013; Pritzkow et al., 2013) presumably having substantial impact on the two major functions of the xylem and consequently also wood density.

In the field of dendroclimatology the most frequently used parameters are tree-ring width (TRW) (e.g. St. George, 2014) and maximum latewood density (MXD) (e.g. Schweingruber et al., 1978; Briffa et al., 2002a), whereas other available tree-ring parameters, such as latewood density (LWD), earlywood density (EWD), minimum density (MND), tree-ring density (TRD), earlywood width (EWW) or latewood width (LWW), are rather rarely used (e.g. Cleaveland, 1986; Griffin et al., 2011; Babst et al., 2014; Camarero et al., 2014; Olivar et al., 2015 being notable exceptions). This preference for TRW and MXD has evolved naturally due to technical constraints and prioritization of parameters with documented high sensitivity to climate (e.g. Schweingruber et al., 1978). With the exceptions of some attempts to model aggregates (e.g., Misson et al., 2004; Rathgeber et al., 2005), and to empirically study ontogenetic trends of some of the tree-ring parameters (e.g. Gartner et al., 2002; DeBell et al., 2004), the combined potential of these parameters, as means to widen the perspective and explore general phylogenetic and geographical patterns of inter-annual tree growth, is generally neglected. Furthermore, a tree-growth centric use of the above-mentioned tree-ring parameters would benefit from meaningful information about the underlying anatomical basis of them. In a general sense, the anatomical basis of tree-ring parameters are conceptually known; ring width is largely a function of the number of tracheids produced each season, and wood density is a function of the average size and the amount of wall material fixed in the tracheids (Vaganov et al., 2006). At intra-annual timescales, density increases from earlywood to latewood mainly as a function of diminishing sizes of tracheids (e.g. Rathgeber et al., 2006; Cuny et al., 2014). However, the specific contributions of cell size and wall dimensions at inter-annual time-scales are only partly

explored. The inter-annual variability of latewood density has mainly been attributed to fluctuations in cell-wall material, (Wang et al., 2002; Vaganov et al., 2006), however there are no investigations, to our knowledge, of the anatomical basis for the inter-annual fluctuations in earlywood density. This leads to the question whether tracheid size or the amount of tracheid wall material dominates the inter-annual variability in earlywood density, and we emphasize that the relative importance of the different anatomical features may be different in earlywood and latewood due to their fundamentally different functions, that are conductivity and mechanical support respectively.

On this background, we postulate the following hypotheses: (1) the inter-annual variability in earlywood density in conifers is mainly governed by fluctuations in the sizes of the tracheids (cross-sectional tracheid area (TA)), which indirectly influence lumen sizes and sap flow. (2) A re-examination of the inter-annual variability in latewood density will verify that it is mainly governed by fluctuations in the incorporated cell wall material (cross sectional cell wall area (CWA)) to enhance mechanical support.

To address these hypotheses, we first present a comprehensive analysis of a network of tree-ring width and density data covering mainly the boreal part of the Northern Hemisphere to establish general patterns of inter-annual growth variability. Second we conduct corresponding analyses using a smaller wood anatomical dataset to confirm the presence of similar patterns. The corresponding anatomical analyses are conducted by deriving density and width features from cell anatomical features, thus establishing an interface between tree-ring data and wood anatomical data. Third we perform a series of sensitivity analyses of the cell anatomical features to identify their contribution in determining wood density to address our hypotheses. Finally, we discuss the implications of the hypothesized contributions of cell size and wall dimensions to wood densities to promote our understanding of how tree-ring growth parameters are inter-connected but also environmentally controlled. Further, we discuss how the identification of the anatomical basis of density can help to assess inter-annual fluctuations in anatomical properties and the associated impacts on xylem functionality.

Materials and methods

Northern Hemispheric network of tree-ring data

This study includes ring width and density datasets retrieved from the International Tree Ring Data Bank (ITRDB, http://www.ncdc.noaa.gov/paleo). The included datasets were selected by screening for sample sites where most of the parameters: MXD, LWD, MND, EWD, LWW, EWW and TRW (Fig. 1) were measured.

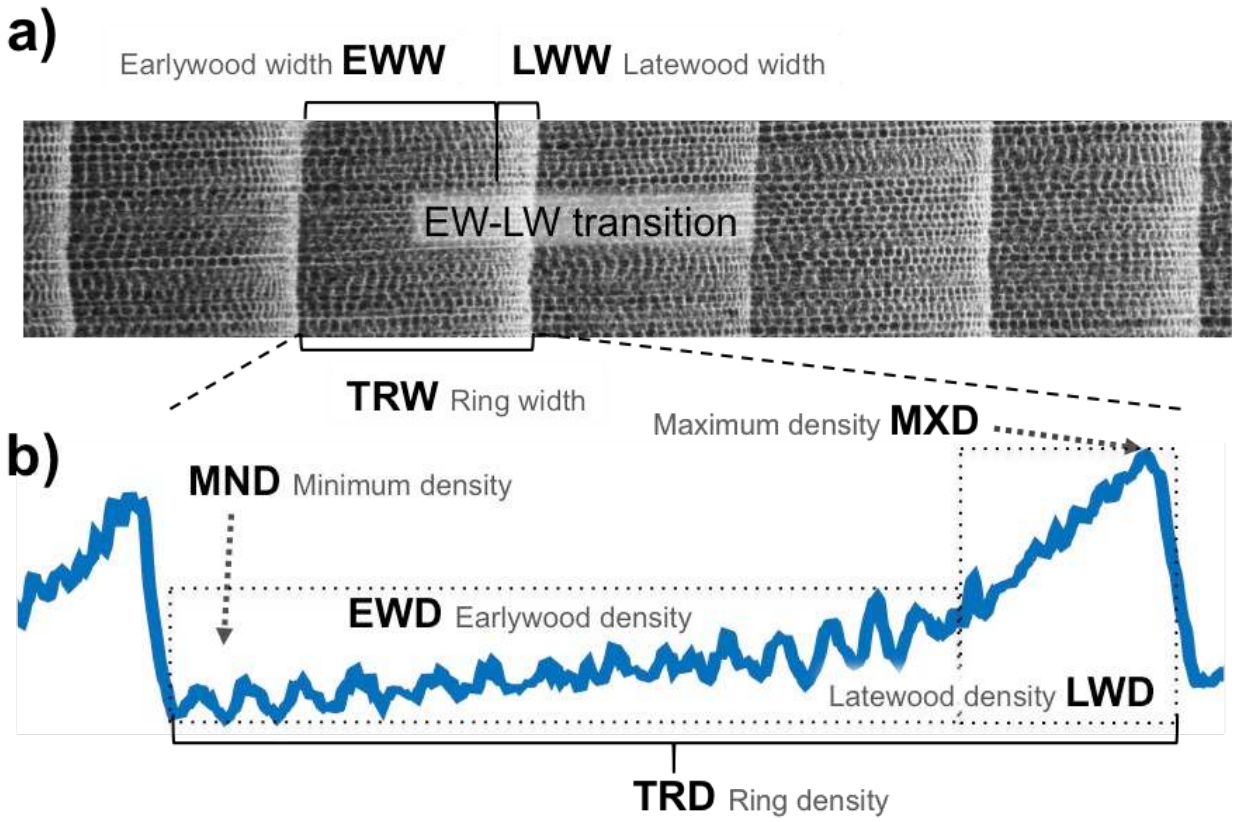

Figure 1. a) X-ray photograph of tree rings in a specimen of *Picea engelmanii*, where the ring-width parameters: earlywood width (EWW), latewood width (LWW) and ring width (TRW) are illustrated. b) X-ray wood density profile. From the intra-annual profile the parameters minimum density (MND), earlywood density (EWD), tree-ring density (TRD), latewood density (LWD) and maximum density (MXD) were derived. In the NH network, the transition from earlywood to latewood is defined as the 50% threshold between MND and MXD, and radial profile analysis step size ~10µm.

Moreover the TRD parameter (not archived) was computed as:

$$TRD_t = \left[\left(EWD_t \times \frac{EWW_t}{TRW_t}\right) + \left(LWD_t \times \frac{LWW_t}{TRW_t}\right)\right] \quad \text{Eqn 1}$$

where *t* refers to the *year* of each tree-ring property. In the following we often use the terms latewood density for LWD and MXD, earlywood density for MND and EWD, ring density for TRD and ring width for EWW, LWW and TRW. The Northern Hemispheric network of tree-ring data (NH-network) largely consists of boreal conifers, targeted by Fritz Schweingruber and colleagues during the last three decades of the 20th century for temperature reconstruction purposes (e.g. Briffa et al., 2002b). See Fig. 2 for geographic distribution of chronologies and genera, and Supporting Information, Notes S1-S2 and Figs. S1-S2 for further details on the NH-network.

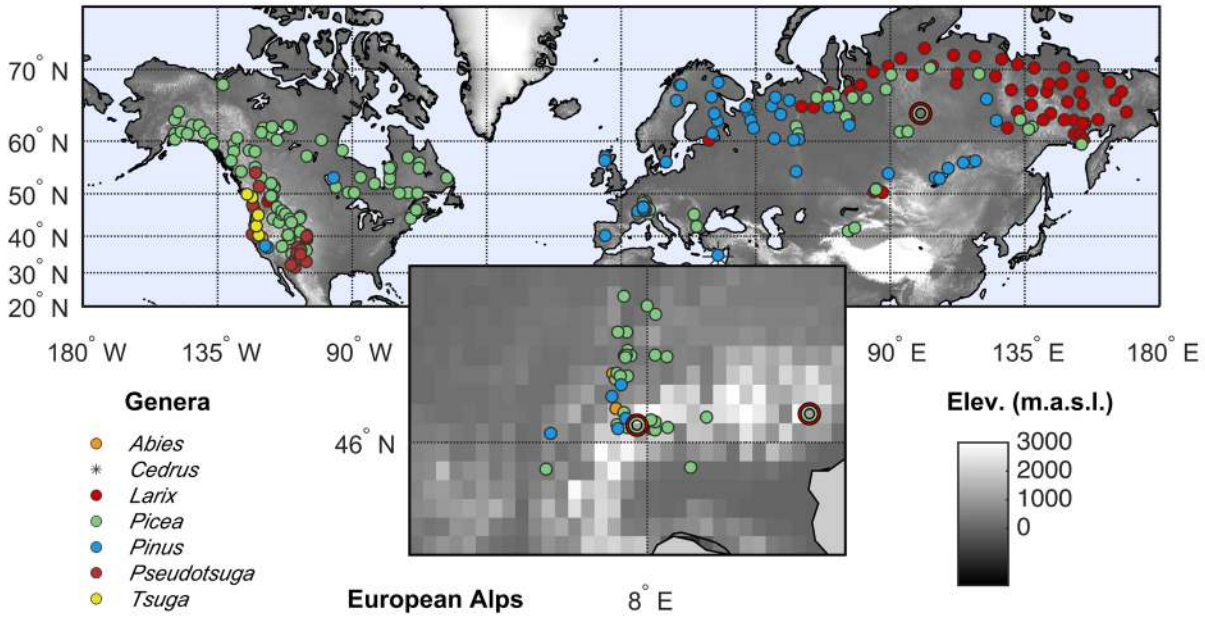

Figure 2. Map displaying the geo referenced site locations of the 349 tree-ring chronologies in the NH-network. Colours identify the genus. The geo referenced site locations of the 8 anatomical datasets are displayed as open circles, to separate between the NH-network data and the anatomy data (the double band of green and red mean that all sites have both *Picea Sp.* and *Larix Sp.*).

Analyses in this study focused on inter-annual to decadal timescales. Therefore longer timescale variance in the tree-ring data, such as the biological age trends, or lower-frequency variability driven by internal or external factors (including climate), was removed through standardization (Fritts, 1976). Cubic smoothing splines with a 50% frequency response cutoff at 35-years (Cook & Peters, 1981) were fitted to each individual tree-ring series. The splines were either divided into (ratios for ring widths) or subtracted from (residuals for densities) the tree-ring series to

206 produce indices (Cook & Peters, 1997). The resulting indices were averaged arithmetically into
207 tree-ring chronologies, i.e. time-series with annually dated tree-ring information. The common
208 signal, i.e. a synchronous behavior in each chronology's tree-ring series through time, was
209 assessed with the *Rbar* statistic (Wigley et al., 1984; Fig. S3). The inter-relationship among NH-
210 network parameters was investigated with pair-wise Pearson correlations for each site and
211 species over the full length of each chronology.
212
213 ## Climate data and climate correlations
214 The climate correlations in the NH-network were calculated using the CRU TS3.22, 0.5° gridded
215 monthly temperature and precipitation data spanning 1901-2013 (updated from Harris et al.,
216 2014). The dataset was detrended analogously to the tree-ring data to extract high-frequency
217 variations, to match the limited frequency range of the detrended tree-ring data and to reduce
218 probabilities of spurious correlations due to trends in the datasets. We used the MATLAB
219 function seascorr, developed by Meko et al. (2011), to quantify the climate signals in the tree-
220 ring data. Pearson correlation coefficients were computed between each parameter chronology
221 (for each site and species) and the temperature data from the nearest grid point. The relationships
222 were assessed using monthly data over a 19-month window spanning from April of the year prior
223 to ring formation up to October of the year of growth. Correlations were computed for the period
224 of maximum overlap between each site chronology and the observational climate record.
225 Although a common period would provide increased consistency, the maximum overlap was
226 chosen to attain as robust correlations as possible as the common period in our NH-network only
227 spans 1941-1968. Due to an often strong co-variation between temperature and precipitation (e.g.
228 higher warm-season temperatures associated with lower precipitation; Trenberth & Shea, 2005)
229 we computed partial correlations between precipitation and tree-ring data to determine if the
230 confounding covariation of climate parameters is important, but also to determine if moisture
231 alone is limiting for growth.
232
233 Moreover, the broad spatial and phylogenetic behavior of the temperature response across the
234 NH-network was analyzed using a cluster analysis, here the K-Means algorithm (MacQueen,
235 1967). The analysis was based on the correlation matrix quantifying relationships between
236 monthly temperatures and the latewood density records. The clustering was based on the current

year MXD parameter, since it displayed the most significant temperature response. The distance from each observation to the centroid of the cluster (group) was quantified using the Euclidean distance. The optimal number of clusters in the dataset was estimated by means of the gap statistics (Tibshirani et al., 2001) and the silhouette width (Kaufman & Rousseeuw, 1990).

Tracheid anatomical data

The anatomical data used in this study, included features of tracheid radial diameter, cell wall thickness (Fig. 3) and number of tracheid per ring from 8 data sites, see open circles in Fig. 2 for geographic distribution. These data are further described in Notes S4.

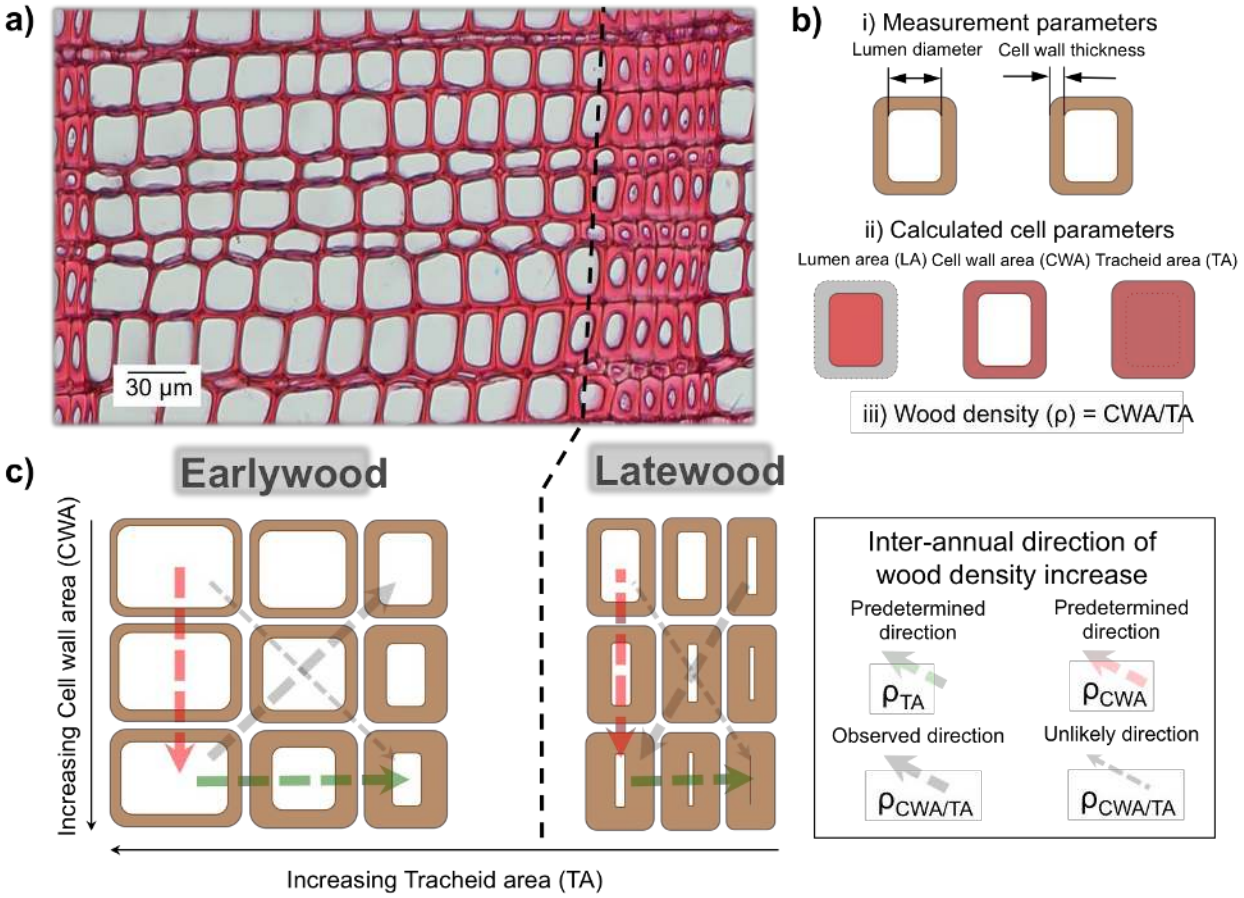

Figure 3. a) Photograph of tracheid anatomy in a specimen of *Pinus sylvestris*, where a dashed line demarcates the earlywood/latewood transition. b) the measured cell anatomical parameters include i) radial lumen diameter (LD) and radial cell wall thickness (CWT) but also the number of cells along the radial distance from beginning of the earlywood to the end of the latewood. From LD and CWT the parameters ii) cell wall area (CWA) and tracheid (TA) were calculated using equations presented in Notes S4. These

parameters are used to calculate relative iii) wood density ρ = CWA/TA. c) Conceptual model of how univariate and bivariate densities change when tracheid area, cell wall area or both are changed respectively. Note the difference between earlywood and latewood, the grey arrows indicating the direction of bivariate density increase. Univariate densities behave in the same way in both early- and latewood, whereas bivariate density ($\rho_{CWA/TA}$) is commonly positively correlated with ρ_{TA} in the earlywood, but does not have to be positively correlated with ρ_{CWA}. $\rho_{CWA/TA}$ is in contrast commonly positively correlated with ρ_{CWA} in the latewood but can be negatively correlated with ρ_{TA} due to the usually small changes in the lumen area, thus defining a functional switch in variability of tracheid anatomy in earlywood and latewood respectively.

The density of conifer wood can largely be determined by two different wood anatomical parameters: cell wall area (CWA) and the tracheid area, the area within the outer dimensions of the tracheid (TA) (Eqn. 2; Fig. 3b; Vaganov et al., 2006). Cell wall area and tracheid area profiles were derived from the tracheid diameters and cell wall thickness measurements using model equations established in Fonti et al. (2013) (Notes S4), at a similar radial step size as has been commonly used in the NH-network (10 microns). From the anatomical profiles we calculated density profiles and extracted parameters such as MXD (cf. $MXD\rho_{CWA/TA}$ with $MXD_{X\text{-}ray}$). The density profiles were calculated as follows

$$\rho_{CWA/TA} = CWA/TA \qquad \text{Eqn 2}$$

where ρ denotes density and thus $\rho_{CWA/TA}$ represents the *bivariate* relative intra-annual wood density profile (Fig. S4a). We conducted similar parameter inter-correlation and climate correlation analyses as was done for the NH-network and compared average broad-scale features from the X-ray density data and the anatomical density data.

To identify the importance of either wall material or cell size for inter-annual variations in wood density, we applied a series of sensitivity analyses, a statistical method that aims at determining the relative influence of each input parameter on a modeled output parameter by alternately holding one input parameter constant. In this study, the modeled output parameter was anatomical wood density, and the input parameters were cell wall area and tracheid diameter. Thus, the analysis involved the calculation of density profiles with equation 2, but also

calculating inter-annual density profiles alternately using an average profile of either cell wall area or tracheid area as follows:

$$\rho_{CWA} = CWA/\overline{TA} \quad \text{Eqn 3}$$

$$\rho_{TA} = \overline{CWA}/TA \quad \text{Eqn 4}$$

where ρ_{CWA} denotes the *univariate* intra-annual wood density, where only cell wall area contributes to the inter-annual variation in density, and ρ_{TA} is the inverse case. Again we extracted the density parameters from the profiles (Fig. S4a-c). Subsequently bivariate and univariate densities were correlated to each other, but also to corresponding widths and to current year temperatures. To describe the results of the sensitivity analysis we henceforth usually refer to the following terminology: r[*x, y*] that denotes the *correlation* between the parameters *x* and *y*. Typically, *x* and *y* refer to widths, bivariate or univariate anatomical densities, or monthly temperature parameters.

Results

Parameter inter-correlation analyses of the NH-network

The inter-correlations between the ring width and density parameters in the NH-network reveal a strongly systematic pattern (Fig. 4).

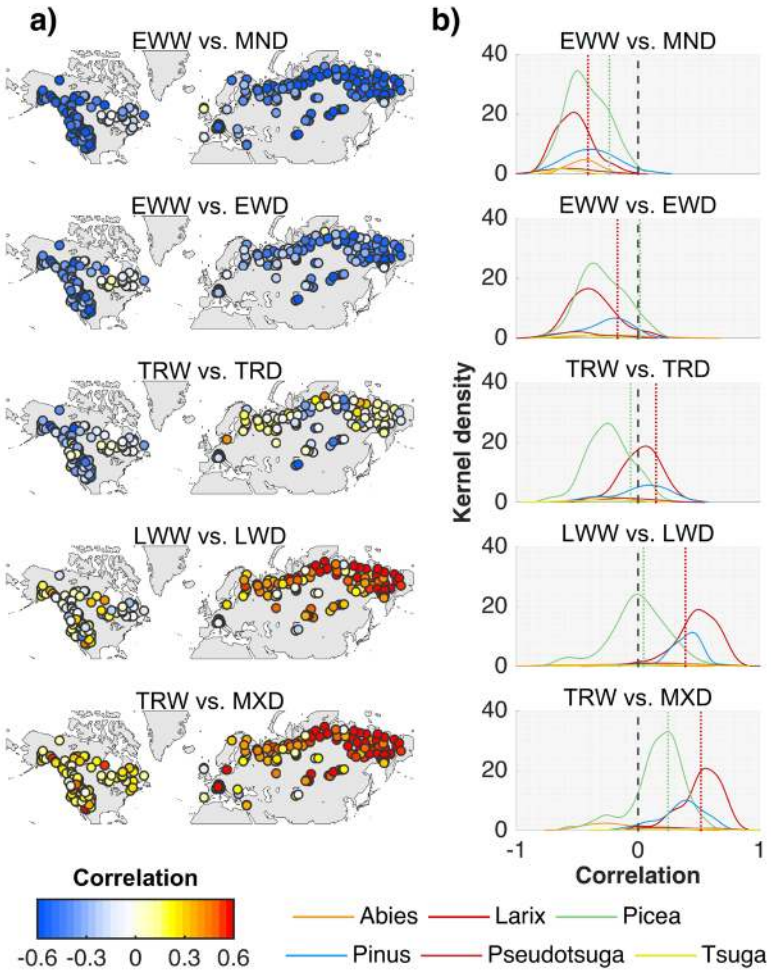

Figure 4. a) Spatial distribution of Pearson correlation coefficients between different pairs of ring width and density parameters in the NH-network. b) Kernel density distributions of correlation coefficients between the same pairs, stratified on genus. Inset red (*Larix sp.*) and green (*Picea sp.*) dotted lines denote the analogue results from the cell anatomical network. Note the shift from negative correlations between earlywood widths and densities to positive correlations between latewood widths and densities, here termed the "EW-LW correlation-sign change". Note also the zonal gradient in strength of correlation coefficients, most prominent for latewood width versus latewood density, termed the "bimodal biogeographic correlation", which coincides with the uneven spatial distribution of the genera *Larix sp.* and *Picea sp.*, also evident from the analogue cell anatomical data analysis.

From a consistently negative association between ring width and earlywood density, there is a modest association with both negative and positive correlations between ring width and ring density, and finally a predominantly positive correlation between latewood density and ring width (Fig. 4). We henceforth refer to this switch in sign of correlations as the "EW-LW correlation-sign change". The inter-correlation analysis also shows that the width parameters

EWW and LWW are usually highly positively correlated to each other, but the earlywood density and latewood density parameters are usually only modestly correlated (Fig. S5).

We also observed a prominent gradient in correlation coefficients of many parameter-pairs, from western North America to Eurasia. The gradient is most pronounced for: r[*ring width, latewood density*] and strongly related to the uneven spatial sampling of *Larix sp.* and *Picea sp.* (Fig. 4b). The gradient feature is henceforth referred to as the "bimodal biogeographic correlation", where *Larix sp.* exhibit a more pronounced "EW-LW correlation-sign change" than *Picea sp.* (Fig. 4b). The "bimodal biogeographic correlation" appears for most parameter-pairs (Figs. 4b and Fig. S5) but is less pronounced for r[*ring width, earlywood density*] or r[EWW, TRW]. The pattern can partly be explained referring to the fact that *Picea sp.* usually displays lower within-chronology series inter-correlation (*Rbar*) (Fig. S3b). That is, *Picea sp.* ring-width series contain a lower degree of common variance, and when noisier chronologies are correlated with chronologies with stronger signal (exhibited within density), the chance of attaining high correlation coefficients is reduced. It is however unlikely that the "bimodal biogeographic correlation" is exclusively related to the lower *Rbar* for *Picea sp.* widths, for at least two reasons: (1) the pattern is not discernible in the correlation between width and density in the earlywood, and, these (negative) correlations are highly significant pointing to a predictable, non-noise driven process in *Picea sp.* ring widths; (2) the pattern is maintained also when correlating only density parameters, for example r[*latewood density, earlywood density*] (Fig. S5). Thus, there likely also exists a systematic anatomical difference that can more comprehensibly explain the "bimodal biogeographic correlation".

Climate correlation and grouping of the NH-network

The climate-growth relationships across the sites and species indicate that temperature is the most important climatic factor in the NH-network (Fig. 5), although weaker but consistent correlations with precipitation are also emerging in late summer for all density parameters at most latitudes (Fig. S6).

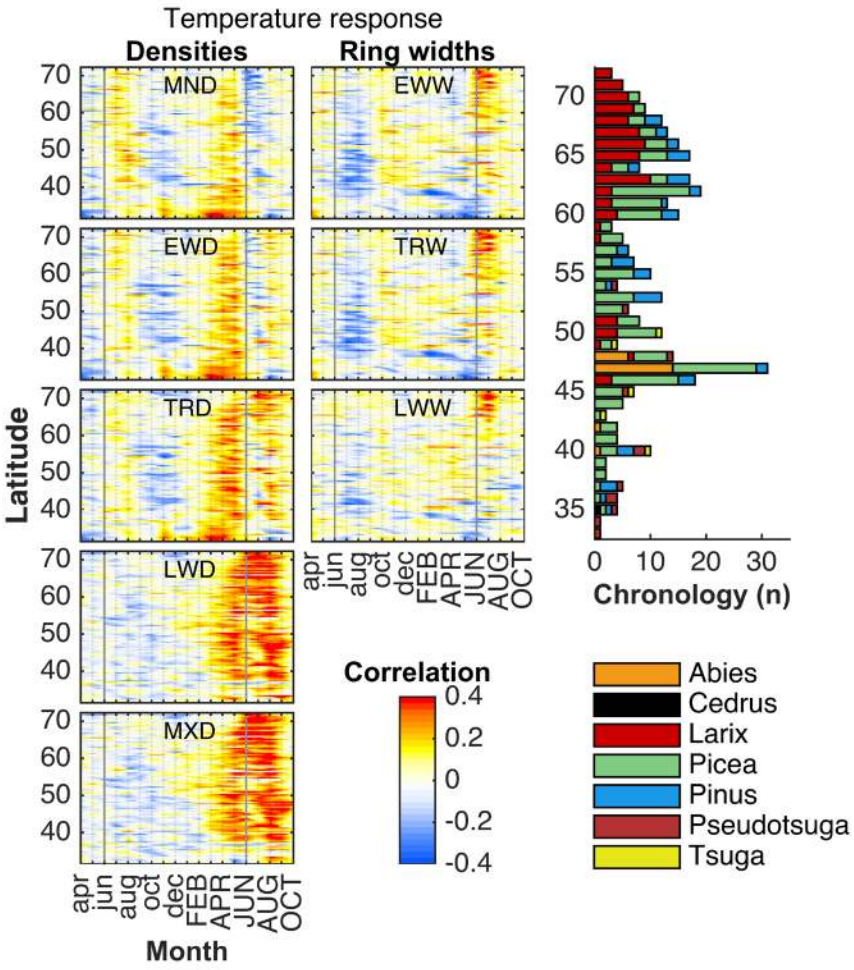

Figure 5. Hovmöller diagrams over temperature – density correlations as a function of latitude. Correlation coefficients were computed between monthly temperatures for the previous (April through December) and current (January through October) growth year and the different NH-network parameters. The horizontal bars indicate chronology replication over the latitudes (averaged over 1° lat. intervals), stratified according to tree-genera with a color-code. Climate data were obtained from the CRU TS3.22 dataset (Harris et al., 2013), from grid points overlaying the chronology locations. Correlations were computed for the period of maximum overlap between each site chronology and the observational climate record. Climate analysis was performed using the Seascorr matlab function (Meko et al., 2011).

The temperature response of the ring-width parameters (Fig. 5) for sites above ~55° latitude is generally positive in mid-summer, and for sites around ~40-55° N, the broad scale signature is a lagged negative correlation with previous years mid- or late summer. Latewood width has reduced lagged correlations in comparison to earlywood width. The temperature correlations of

the density parameters are usually stronger and more consistent over latitude. In the following we explore the wood density temperature interaction in more detail.

The cluster analysis divided the NH-network into five groups with characteristic climate response patterns. Fig. 6 shows the spatial repartition of the sites and species belonging to each cluster, with the average temperature response of the density parameters (see Fig. S7 for complete results).

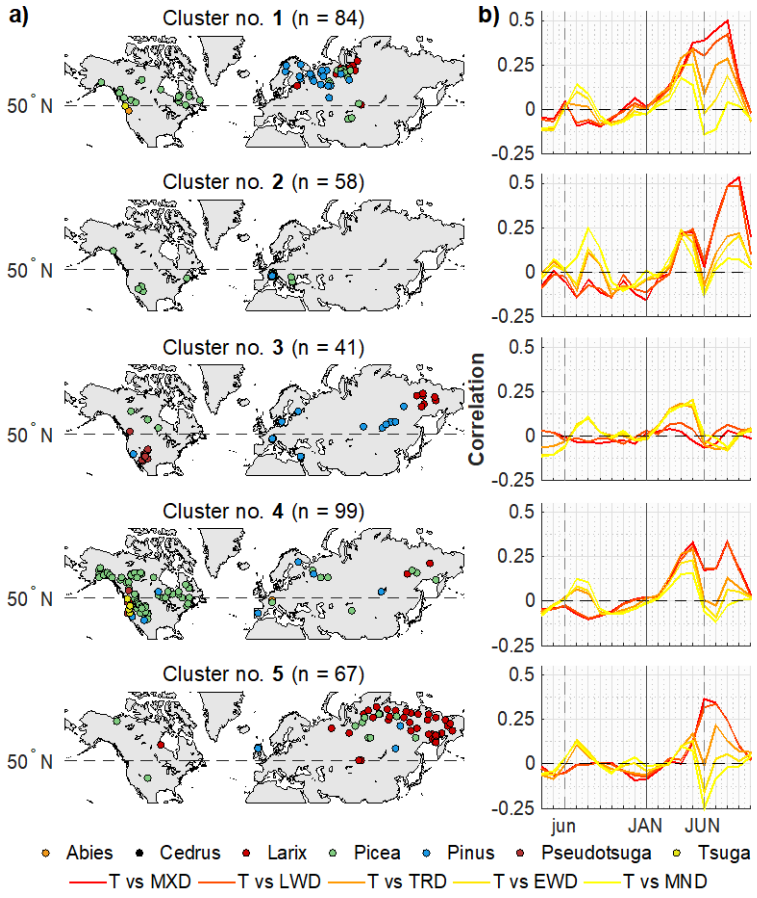

Figure 6. Cluster identification of the NH-network. The grouping was based on the temperature response of the MXD parameter in the period January-October of the current year. a) The spatial groupings of each cluster stratified by genus, and b) the corresponding average temperature correlation of MXD (red), LWD, TRD, EWD and MND (yellow).

Clusters 1, 2, 4 and 5 describe distinct temperature signals, while cluster 3 groups' sites without a clear latewood density temperature correlation. Cluster 1 is predominantly located at high

latitudes or altitudes in Scandinavia, European Russia and in Canada, primarily composed of *Picea sp.*, *Larix sp.* and *Pinus sp.* Its composition is not substantially different from the original fractionation of genera in the entire NH-network (Fig. S7a) and therefore classified as geographically determined. Cluster 2 is composed of lower latitude sites, located mainly throughout the Alps, over-represented by the genera *Picea sp.* and *Abies sp*. Cluster 4 suggests a more or less genus-specific separation predominantly constituted by *Picea sp.* scattered across the North American continent. The majority of the sites in cluster 5 are found over Siberia, predominantly composed of *Larix sp.*

The temperature correlation for each cluster reveals striking complexities and similarities, both among clusters but also among parameters (Fig. 6). The correlation structure is broadly characterized by a reliable positive correlation with current year spring (March-May), which is strongly dampened for all parameters at most sites (or even negative for the MND parameter) in the mid summer (June-July), here termed the "mid-summer decline" (Figs. 5 and 6). Late summer is again characterized by positive correlations, particularly when gradually moving from the earlywood to the latewood density parameters. Furthermore, the earlywood densities show systematic lagged correlations with previous year late summer temperatures. The lagged correlations are increasingly dampened moving to ring density and are largely absent in the latewood density parameters. These patterns are observed, albeit to varying extent, in all of the five clusters (Fig. 6). However, the northernmost sites (Fig. 5), or cluster 5 (Fig. 6), do not indicate a "mid-summer decline" in the MXD parameter. Moreover, the southernmost earlywood density site-chronologies (Fig. 5) display more prominent positive spring temperature signals starting already in February, accompanied by an extended period of negative precipitation signals from previous October to current June (Supporting Information, Fig. S6).

Validation of anatomical dataset

Moving from the X-ray derived density data to the cell anatomy derived density data, the same broad-scale features as described above were observed (Fig. 7a and 8 upper panel).

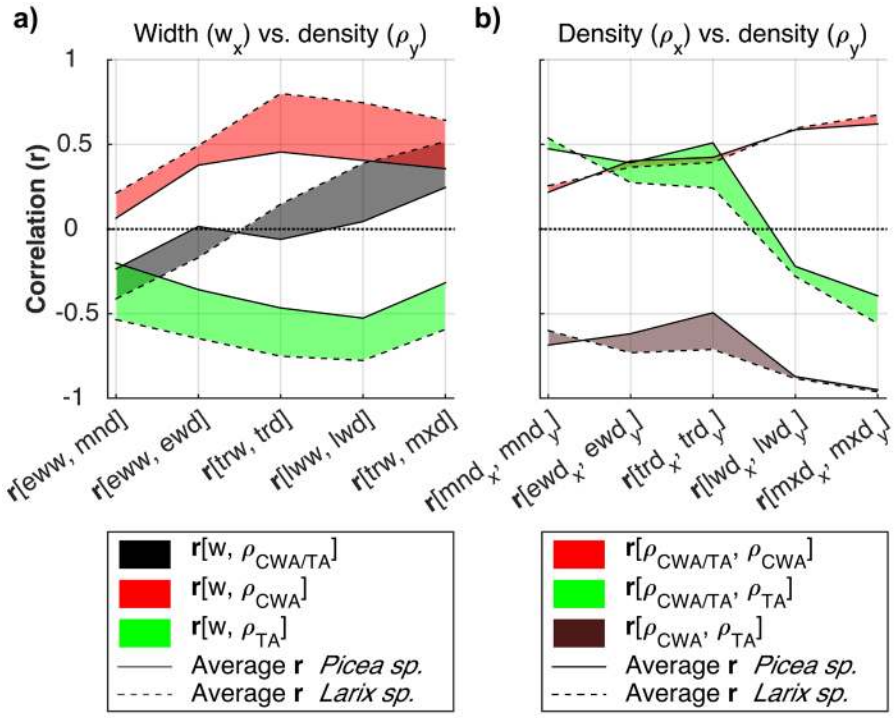

Figure 7. a) The average development of correlation coefficients between different bivariate density parameters ($\rho_{CWA/TA}$) and corresponding widths from the cell anatomical dataset in black dashed (*Larix sp.*, $n = 3$) and solid (*Picea sp.*, $n = 5$) lines. The grey field is the difference between the two genera averages. This depicts the phenomenon termed "EW-LW correlation-sign change" which refers to the fact that earlywood width is negatively correlated to earlywood density, and latewood width and ring width are positively correlated to latewood density. In red dashed and solid lines, same as in black but $\rho_{CWA/TA}$ is replaced by univariate density (ρ_{CWA}) where only CWA contribute to inter-annual density variability. In green dashed and solid lines, ρ_{CWA} is replaced for ρ_{TA} where only TA contribute to inter-annual density variability. b) Red and green, same as in a) but here the widths are replaced for $\rho_{CWA/TA}$. In brown, ρ_{CWA} and ρ_{TA} are correlated against each other.

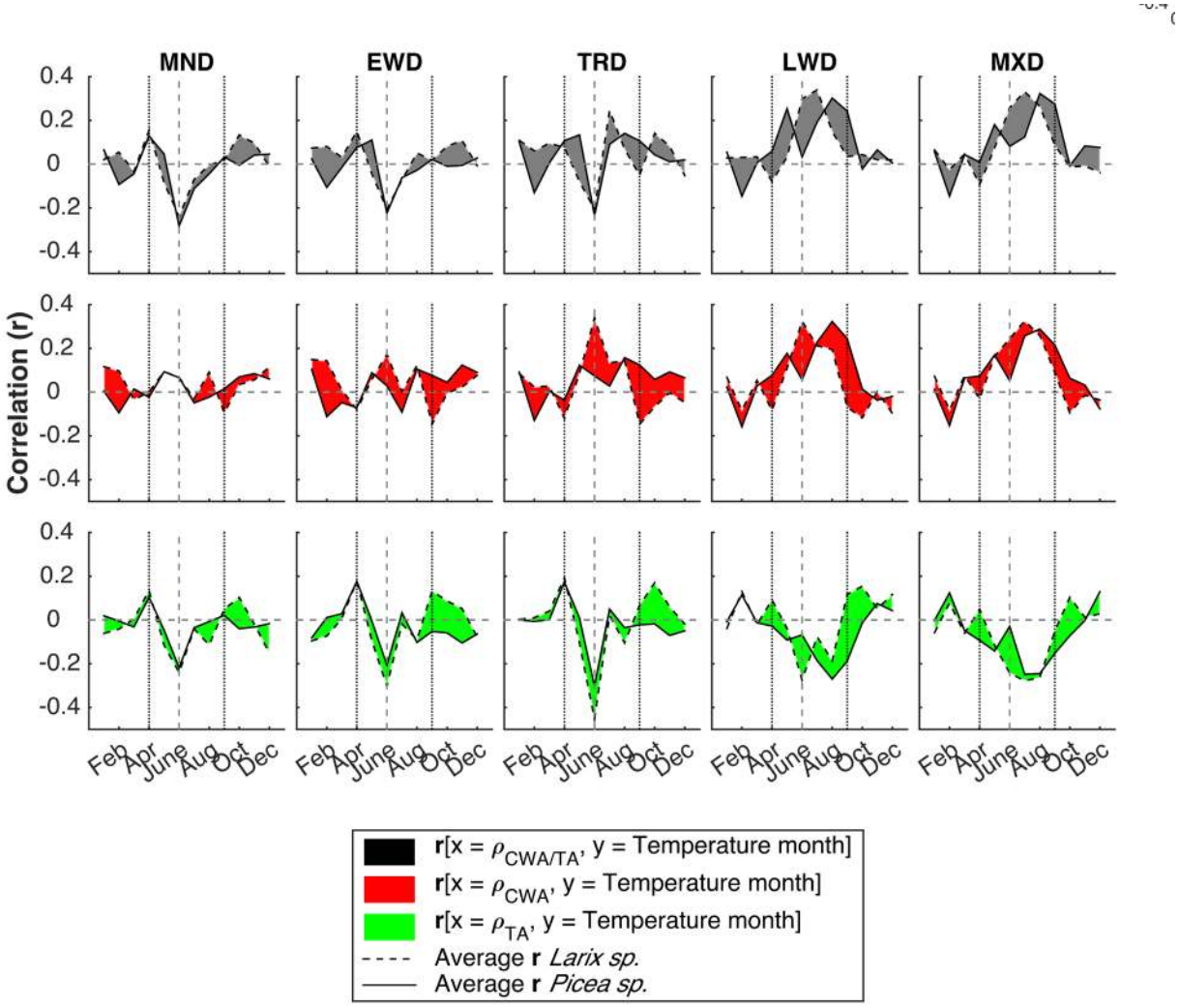

Figure 8. Temperature correlations of different bivariate density parameters ($\rho_{CWA/TA}$) in black, the upper panel. The grey field is the difference between dashed (*Larix sp.* average) and solid (*Picea sp.* average) lines. In red, the mid panel, same as in black but $\rho_{CWA/TA}$ is replaced by univariate density (ρ_{CWA}) where only CWA contributes to inter-annual density variability. In green dashed and solid lines, ρ_{CWA} is replaced for ρ_{TA} where only TA contributes to inter-annual density variability. Correlations were computed between monthly temperatures from January through December and the different density parameters minimum density (MND), earlywood density (EWD), tree-ring density (TRD), latewood density (LWD) and maximum latewood density (MXD). Climate data were obtained from the CRU TS3.22 dataset (Harris et al., 2013), from grid points overlaying the chronology locations and correlations were computed for the period of maximum overlap between each site chronology and the observational climate record.

To summarize, (1) the "EW-LW correlation-sign change" (Fig. 7a) is a prominent feature in the anatomical data, (2) the "bimodal biogeographic correlation" is also represented by the stronger "EW-LW correlation-sign change" in *Larix sp.* (Fig. 7a), (3) the temperature correlation is very similar to the NH-network results, even featuring a pronounced latewood density "mid-summer decline" for *Picea sp.* but not for *Larix sp.* (Fig. 8 upper panel). The only discrepancy between the cell anatomical dataset and tree-ring dataset is the lack of a previous year lagged temperature correlation for the earlywood anatomical densities (results not shown).

Sensitivity analyses of the tracheid-anatomy's influence on wood density

We find ring width measurements are consistently negatively correlated with the univariate tracheid area density (r[*width,* $\rho_{\mathbf{TA}}$] < 0). Furthermore, we find positive coefficients for r[*width,* $\rho_{\mathbf{CWA}}$] (Fig. 7a). Thus both univariate versions of density lack the "EW-LW correlation-sign change". To attain an "EW-LW correlation-sign change" in the observed direction (Fig. 4) we must then infer that tracheid area dominates the variability in earlywood densities, whereas cell wall area is the primary control on the latewood density.

The bivariate density is positively correlated with the univariate cell wall area density (r[$\rho_{CWA/TA}$, $\rho_{\mathbf{CWA}}$] > 0) throughout the entire tree-ring and increasing in strength moving from earlywood to latewood. In contrast, r[$\rho_{CWA/TA}$, $\rho_{\mathbf{TA}}$] is positive only in the earlywood becoming negative in the latewood (Fig. 7b) and absolute values of correlation coefficients are rather unchanged, being higher than r[$\rho_{CWA/TA}$, $\rho_{\mathbf{CWA}}$] only in the earlywood. This again suggests that the earlywood is dominated by fluctuations in tracheid area, however not entirely excluding the role of cell wall area. The situation is more complex in the latewood. The fact that the r[$\rho_{CWA/TA}$, $\rho_{\mathbf{TA}}$] was negative in the latewood means that we counter-intuitively observe a bivariate density increase when the cell size is increased. The finding infers an even greater increase in cell wall area that compensates fluctuations in tracheid area. This is supported by the nearly constant lumen size in the latewood (Fig. S8). Fig. 3c conceptualizes these inter-annual anatomical differences between earlywood and latewood density.

The temperature correlation of the univariate tracheid area density (r[*temperature,* $\rho_{\mathbf{TA}}$]) is almost identical with the r[*temperature,* $\rho_{CWA/TA}$] in the earlywood parameters (cf. the negative June correlation, Fig. 8, not observed for the r[*temperature,* $\rho_{\mathbf{CWA}}$]). In contrast, in the latewood,

462 *r*[*temperature,* ρ_{CWA}] is almost identical with the *r*[*temperature,* $\rho_{CWA/TA}$]. However, the
463 *r*[*temperature,* ρ_{TA}] is an almost perfect mirror image of the *r*[*temperature,* $\rho_{CWA/TA}$].
464
465 Overall, these results indicate that earlywood density is rather controlled by fluctuations in
466 tracheid size, whereas the fluctuations in latewood density are more difficult to disentangle due
467 to the high degree of collinearity between tracheid area and cell wall area (Fig. 7b).
468

469 ## Discussion

470 In this study we jointly assessed quantitative wood anatomy and tree-ring data, to disentangle the
471 contribution of different anatomical features (cell size and cell-wall dimensions) to inter-annual
472 earlywood and latewood density. In the NH-network, that provide the broad overview in this
473 study, we found contrasting associations among tree-ring parameters moving from earlywood to
474 latewood and intricate correlations with climate (Figs. 4-6). Moving to the detail of the anatomy
475 (the microstructure of tree-ring data), we confirmed that the large-scale patterns were compatible
476 with the results found for the density and width derived from the anatomical datasets (Figs. 7-8).
477 This enabled us to study the association between tracheid-anatomy information and tree-ring
478 data. It is important to note that the confirmed patterns in the anatomical data could have been
479 easily missed or dismissed without the support of the NH-network, high-lighting the benefit of
480 our broader approach.
481
482 In the anatomical dataset we found support for the first hypothesis, that earlywood density in
483 conifers is mainly governed by fluctuations in tracheid size. However, we could not confirm or
484 reject the second hypothesis, that the latewood density is mainly governed by fluctuations in the
485 incorporated cell wall material. Our results do therefore not fully support that cell wall material,
486 and not cell size, dominates the inter-annual variability in latewood densities (e.g. Vaganov et
487 al., 2006; Wang et al., 2002). We rather found that such a distinction is unnecessary because
488 larger cells are also associated with proportionally more wall material: an almost perfect co-
489 variation. In the following we will discuss the implications of this shift in relative importance of
490 cell anatomical features for wood density, and use it to 1) decipher the inconsistent associations
491 among tree-ring parameters as well as the complex temperature responses of the density

parameters, and 2) how this shift can be exploited for interpretations of inter-annual variability in anatomical properties and associated xylem functionality.

Tracheid anatomy explains tree-ring data relationships

We have shown that tracheid area is the main anatomical feature determining earlywood density. Tracheid area has a negative influence on density (Fig. 3c), but is positively correlated with the number of cells per ring (Fig. S9), which is the main determinant of ring width (Vaganov et al., 2006). Therefore, when correlating earlywood density and ring width it is very likely to attain a negative relationship, as observed in this study (Fig. 4). The relevance of tracheid area in the earlywood density is reduced in the latewood, but also, the size of the tracheid area has here a positive association with latewood density (cf. conceptual model of earlywood and latewood density in Fig. 3). Since the contributions from both cell wall area and tracheid area to latewood density appear to be positive, and both cell wall area and tracheid area are positively correlated with number of tracheids (Fig. S9), it is very likely to attain positive correlations between width and density, as observed in this study, (Fig. 4). Thus, the "EW-LW correlation-sign change", is likely driven by the fact that the earlywood and latewood components maintain this fundamental shift in relative importance of cell anatomical features.

Inferring structure and functionality using tree-ring data

Further capitalizing on the joint use of anatomical data and tree-ring data, our results are also relevant because they provide evidences for a causal link between a widely used ecological and environmental proxy (density) (Chave et al., 2009; Wilson et al., 2016; Stoffel et al., 2015) with its fundamental structural-functional origin (anatomy).

The consistency of our discoveries (>90% of sites have significant negative correlations between ring width and earlywood density ($\alpha < 0.05$)) implies an almost universal mode of coupled environmental response of earlywood width and earlywood density. The hydraulic efficiency in conifers is linearly increased with the number of conduits or cells (~earlywood width), and it is exponentially increased with the lumen area of the cells (Sperry et al., 1994). Because earlywood density is mainly controlled by changes in tracheid sizes (tracheid area and lumen area are interchangeable in the earlywood; i.e. almost perfectly correlated (Fig. S9)), and changes in tracheid size have exponential impact on conductivity, density and width should be interesting

proxies for inter-annual variations in conductivity because of the currently superior replication and geographical coverage of tree-ring data. This prospect has previously also been suggested by Dalla-Salda et al., (2011), which conducted their study on 27 juvenile plantation Pseudotsuga menziezii trees.

Furthermore, there is also a near universal mode of coupled environmental response of latewood width and latewood density (>80% of sites show significant positive correlations between ring width and latewood density ($\alpha < 0.1$)). The mechanical function of the xylem is promoted by increased deposition of wall material (Chave et al., 2009) and increased number of latewood cells. By maintaining the shift in relative importance of tracheid features moving from the earlywood to the latewood, the same environmental conditions can consecutively promote the conductivity of the earlywood *and* the mechanical function of the latewood. The density in the latewood may thus compensate any impairment in mechanical function caused by the earlywood, complying with universal plant functional trade-offs (Baas et al., 2004).

Environmental responses in functionality of either earlywood or latewood anatomy, have to our knowledge, only been established at local scale (e.g. Bryukhanova and Fonti, 2013; Castagneri et al., 2015; Pritzkow et al., 2013). In this study we indirectly demonstrate, for the first time, that conifers may increase their hydraulic efficiency in the earlywood, as well as their mechanical strength in the latewood, as a response to the same environmental conditions. Interestingly, these modes of responses are largely independent of phylogeny or prevailing climate regimes in the Northern Hemisphere.

Anatomical basis and sequential formation explain differences in temperature responses

Tracheid size, the major determinant of earlywood density, is a function of turgor pressure and hormonal control through cell wall relaxation occurring during the phase of cell enlargement (Cosgrove, 1985). For trees in cold-limited environments, conductivity, expressed by lumen area, is increased with temperature (Petit et al., 2010). The apparent paradox that temperature could drive the tracheid enlargement can perhaps be explained by that water availability generally is not a limiting factor in cold environments. This is indirectly observed in this study, where responses to precipitation are modest and responses to temperature are pronounced (Figs. 5 and S6). Because the temperature sensitive cell size has a negative influence on earlywood density,

554 the major response is negative in mid-summer, coinciding with the period when most of the cells
555 are formed and matured (e.g. Seo et al., 2008; Cuny et al., 2014). Since the tracheid area does not
556 exclusively determine earlywood density, there is likely also some influence by the cell wall
557 area. The positive temperature response preceding the negative temperature response, also found
558 as a lagged correlation in the previous year, is presumably best explained as a wall deposition
559 signal.
560 In the latewood, where both tracheid area and cell wall area are positively influence density, we
561 do not observe, and should not expect, negative responses to temperature. Studying the positive
562 temperature correlations for the density parameters (Figs. 5 and 6), it is clear that their timing
563 does not fully match with the timing of ring/cell formation (e.g. Seo et al., 2008; Cuny et al.,
564 2014). Earlywood densities show consistently positive responses to the previous year. Latewood
565 densities have pronounced responses to early spring. The cell wall contribution to wood density,
566 regardless if in early- or latewood, must therefore be realized by capitalizing on resources
567 collected during an extended period, spanning also prior to the time of formation. This is
568 supported by Kagawa et al. (2006) that report that earlywood formation strongly rely on
569 photosynthates stored from the previous year in *Larix gmelinii*, and by Kuptz et al., (2011) that
570 concludes that also older pools of photosynthates are used for secondary stem growth in *Picea*
571 *abies.* Vaganov et al., (2009) also find carry-over effect in $\delta^{13}C$ of the latewood the previous year
572 to earlywood the current year in *Picea abies* and *Pinus sp*. Even though the resource-use from an
573 extended period is compatible with latewood results from the anatomical dataset, the previous
574 year lagged response in the earlywood was not detectable (Fig. 8). This absence of lagged
575 correlation in the anatomical data does however not rule out a lagged use of resources from
576 previous year to build earlywood tissue, but it dilutes the support.
577 In conclusion, the differentiated relative importance of anatomical features causes major
578 differences between the temperature responses of earlywood and latewood density. A second
579 inconclusive difference is that the earlywood density could also depend on previous year's
580 reserves.
581

582 ## Similarities in wood density temperature responses are still elusive

583 In addition to distinct differences, we found conspicuous similarities in temperature signals of
584 earlywood and latewood densities. These are represented by synchronous positive early season

responses followed by the "mid-summer decline" in the latewood, which is negative for the earlywood (Fig. 6). In the earlywood we conclude that this temporal evolution of correlation coefficients is created by the opposing influence from the positive cell wall signal and the negative cell size signal. We do not rule out that also in the latewood such a mechanism is present. However, this feature was not directly supported by our analyses, because ρ_{CWA} also display a "mid-summer decline" (Fig. 8). Recurring mid-summer temperature-induced drought, during which high temperatures become a stress factor is also questionable, because density is slightly negatively affected by increased precipitation just after mid-summer (Fig. S6), and thus difficult to reconcile with mid-summer temperature stress. The role of resource allocation is also inconclusive. A depletion of mid-summer assimilates by concurrent cell division and cell enlargement, may leave only resources accumulated in early and late summer for latewood formation. This could explain reduced correlations with mid-summer temperatures. Cuny et al., (2015), found that the cell division and enlargement processes require astonishingly small amounts of carbon, compared to the wall deposition process, and a depletion when assimilation is at its peak (Bourdeau, 1959) is therefore unlikely.

Concluding remarks

We found a transition in relative importance – from cell size towards cell wall dimensions – that drive distinct year-to-year variability of earlywood and latewood density in Northern Hemisphere conifers, respectively. This transition explains the relationships between radial stem-growth and wood density; earlywood densities are negatively correlated with ring widths while latewood densities are positively correlated with ring widths. It also explains the complex temperature responses of wood density (notably varying intra-seasonally in strength or even sign). These findings substantially improve our understanding of inter-annual variations of conifer growth and are vital for the interpretation of existing and future temperature reconstructions relying on the MXD parameter (e.g. Briffa et al., 2002; Wilson et al., 2016).

Furthermore, because we could so easily integrate the anatomical data patterns with the phylogenetically and geographically diverse tree-ring data patterns, and identifying a mechanism explaining why we observe these patterns, we conversely infer that the anatomy of earlywood and latewood tissues vary according to some simple universal rules. a) The year-to-year

variability of earlywood tissue is dominated by variation in cell size, which support hydraulic-functional responses to climate. b) In contrast, the year-to-year variability of latewood tissue is more dependent on cell wall variations, which permit mechanic-functional responses to climate. By combining the detailed anatomy data with the large-scale tree-ring data, we illustrate how Northern Hemisphere conifers organize investments in earlywood and latewood tissue, to continuously guarantee an adequately balanced and sustainable functioning of the xylem.

Acknowledgements

This work was mainly funded by the Swiss National Science Foundation (grants iTREE CRSII3_136295 and P300P2_154543). MB was supported by the Russian Scientific Foundation (the project #14-14-00219). HEC was supported by the Swiss National Science Foundation (grant no. 160077, CLIMWOOD). RP was supported by the Swiss National Science Foundation (grant no. 150205, LOTFOR). GvA was supported by a grant from the Swiss State Secretariat for Education, Research and Innovation SERI (SBFI C14.0104). We thank two anonymous referees for their thoughtful and constructive critique, and also the numerous researchers who have contributed their tree-ring data to the International Tree-Ring Data Bank, IGBP PAGES/World Data Center for Paleoclimatology, NOAA/NCDC Paleoclimatology Program; Boulder, Colorado.

Author Contribution

JB, KS, PF, GvA and DCF planned and designed the research; JB and KS performed the research; FS, PF, GvA, MB, MC and DC provided data; JB and KS wrote most of the manuscript but with substantial contributions from FS, PS, GvA, MVB, HEC, MC, DC and DCF.

References

Baas P, Ewers F W, Davis S D, Wheeler E A. 2004. Evolution of xylem physiology. In: The Evolution of Plant Physiology (eds Hemsley, A.R. & Poole, I.). London, UK: Elsevier Academic Press, 273-295.

Babst F, Bouriaud O, Papale D, Gielen B, Janssens IA, Nikinmaa E, Ibrom A, Wu J, Bernhofer C, Kostner B, et al. 2014. Above-ground woody carbon sequestration measured

from tree rings is coherent with net ecosystem productivity at five eddy-covariance sites. *New Phytol* **201**(4): 1289-1303.

Bourdeau PF. 1959. Seasonal variations of the photosynthetic efficiency of evergreen conifers. *Ecology* **40**(1): 63-67.

Briffa K, Osborn TJ, Schweingruber FH, Jones PD, Shiyatov SG, Vaganov EA. 2002a. Tree-ring width and density data around the Northern Hemisphere: Part 1, local and regional climate signals. *Holocene* **12**(6): 737-757.

Briffa K, Osborn TJ, Schweingruber FH, Jones PD, Shiyatov SG, Vaganov EA. 2002b. Tree-ring width and density data around the Northern Hemisphere: Part 2, spatio-temporal variability and associated climate patterns. *Holocene* **12**(6): 759-789.

Bryukhanova M, Fonti P. 2012. Xylem plasticity allows rapid hydraulic adjustment to annual climatic variability. *Trees* **27**(3): 485-496.

Camarero JJ, Rozas V, Olano JM, Fernández-Palacios JM. 2014. Minimum wood density of *Juniperus thuriferais* a robust proxy of spring water availability in a continental Mediterranean climate. *Journal of Biogeography* **41**(6): 1105-1114.

Castagneri D, Petit G, Carrer M. 2015. Divergent climate response on hydraulic-related xylem anatomical traits of *Picea abies* along a 900-m altitudinal gradient. *Tree Physiol* **35**(12): 1378-1387.

Chave J, Coomes D, Jansen S, Lewis SL, Swenson NG, Zanne AE. 2009. Towards a worldwide wood economics spectrum. *Ecol Lett* **12**(4): 351-366.

Cleaveland MK. 1986. Climatic response of densitometric properties in semiarid site tree rings. *Tree-Ring Bulletin* **46**: 13-29.

678 **Cook ER, Peters, K.** The smoothing spline: a new approach to standardizing forest interior tree-
679 ring width series for dendroclimatic studies. *Tree-Ring Bulletin* **41**: 45-53.
680
681 **Cosgrove DJ. 1993.** Water Uptake by Growing Cells: An Assessment of the Controlling Roles
682 of Wall Relaxation, Solute Uptake, and Hydraulic Conductance. *International Journal of plant*
683 *Sciences* **154**(1): 10-21.
684
685 **Cuny HE, Rathgeber CB, Frank D, Fonti P, Fournier M. 2014.** Kinetics of tracheid
686 development explain conifer tree-ring structure. *New Phytol* **203**(4): 1231-1241.
687
688 **Cuny HE, Rathgeber CB, Frank D, Fonti P, Makinen H, Prislan P, Rossi S, Del Castillo**
689 **EM, Campelo F, Vavrcik H, et al. 2015.** Woody biomass production lags stem-girth increase
690 by over one month in coniferous forests. *Nat Plants* **1**: 15160.
691
692 **Dalla-Salda G, Martinez-Meier A, Cochard H, Rozenberg P. 2011.** Genetic variation of
693 xylem hydraulic properties shows that wood density is involved in adaptation to drought in
694 Douglas-fir (*Pseudotsuga menziesii* (Mirb.)). *Annals of Forest Science* **68**: 747-757.
695
696 **DeBell D S, Singleton R, Gartner B L, Marshal D D. 2004.** Wood density of young-growth
697 western hemlock: relation to ring age, radial growth, stand density, and site quality. *Canadian*
698 *Journal of Forestry* **34**: 2433-2442.
699
700 **Fonti P, Bryukhanova MV, Myglan VS, Kirdyanov AV, Naumova OV, Vaganov EA. 2013.**
701 Temperature-induced responses of xylem structure of *Larix sibirica* (*Pinaceae*) from the Russian
702 Altay. *Am J Bot* **100**(7): 1332-1343.
703
704 **Frank D, Esper J, Zorita E, Wilson R. 2010.** A noodle, hockey stick, and spaghetti plate: a
705 perspective on high-resolution paleoclimatology. *Wiley Interdisciplinary Reviews: Climate*
706 *Change* **1**(4): 507-516.
707

Frank D, Reichstein M, Bahn M, Thonicke K, Frank D, Mahecha MD, Smith P, van der Velde M, Vicca S, Babst F, et al. 2015. Effects of climate extremes on the terrestrial carbon cycle: concepts, processes and potential future impacts. *Glob Chang Biol* **21**(8): 2861-2880.

Fritts HC. 1976. *Tree Rings and Climate*. New York: Academic Press INC.

Hacke UG, Sperry JS, Pockman WT, Davis SD, McCulloh KA. 2001. Trends in wood density and structure are linked to prevention of xylem implosion by negative pressure. *Oecologia* **126**(4): 457-461.

Hanewinkel M, Cullmann DA, Schelhaas M-J, Nabuurs G-J, Zimmermann NE. 2012. Climate change may cause severe loss in the economic value of European forest land. *Nature Climate Change* **3**(3): 203-207.

Harris I, Jones PD, Osborn TJ, Lister DH. 2014. Updated high-resolution grids of monthly climatic observations - the CRU TS3.10 Dataset. *International Journal of Climatology* **34**(3): 623-642.

Gartner B L, North E M, Johnson G R, Singleton R. 2002. Effects of live crown on vertical patterns of wood density and growth in Douglas-fir. *Canadian Journal of Forestry* **32**: 439-447.

Griffin D, Woodhouse CA, Meko DM, Stahle DW, Faulstich HL, Carrillo C, Touchan R, Castro CL, Leavitt SW. 2013. North American monsoon precipitation reconstructed from tree-ring latewood. *Geophysical Research Letters* **40**(5): 954-958.

Kagawa A, Sugimoto A, Maximov TC. 2006. 13CO2 pulse-labelling of photoassimilates reveals carbon allocation within and between tree rings. *Plant, Cell and Environment* **29**(8): 1571-1584.

Kaufman L, Rousseeuw PJ. 2009. *Finding groups in data: an introduction to cluster analysis*: John Wiley & Sons New Jersey.

Kuptz D, Fleischmann F, Matyssek R, Grams TEE. 2011. Seasonal patterns of carbon allocation to respiratory pools in 60-yr-old deciduous (*Fagus sylvatica*) and evergreen (*Picea abies*) trees assessed via whole-tree stable carbon isotope labeling. *New Phytol* **191**: 160-172.

Larson PR. 1994. *The vascular cambium. Development and structure*: Springer-Verlag Berlin Heidelberg.

MacQueen J. 1967. Some methods for classification and analysis of multivariate observations. *Proceedings of the fifth Berkeley symposium on mathematical statistics and probability* **1**(14): 281-297.

Meko DM, Touchan R, Anchukaitis KJ. 2011. Seascorr: A MATLAB program for identifying the seasonal climate signal in an annual tree-ring time series. *Computers & Geosciences* **37**(9): 1234-1241.

Misson L, Rathgeber C, Guiot J. 2004. Dendroecological analysis of climatic effects on *Quercus petraea* and *Pinus halepensis* radial growth using the process-based MAIDEN model. *Canadian Journal of Forestry* **34**: 888-898.

Olivar J, Rathgeber C, Bravo F. 2015. Climate change, tree-ring width and wood density of pines in the Mediterranean environments. *IAWA Journal* **36**(3): 257-269.

Petit G, Anfodillo T, Carraro V, Grani F, Carrer M. 2011. Hydraulic constraints limit height growth in trees at high altitude. *New Phytol* **189**(1): 241-252.

Pratt RB, Jacobsen AL, Ewers FW, Davis SD. 2007. Relationships among xylem transport, biomechanics and storage in stems and roots of nine *Rhamnaceae* species of the California chaparral. *New Phytol* **174**(4): 787-798.

Pritzkow C, Heinrich I, Grudd H, Helle G. 2014. Relationship between wood anatomy, tree-ring widths and wood density of *Pinus sylvestris* L. and climate at high latitudes in northern Sweden. *Dendrochronologia* **32**(4): 295-302.

Rathgeber C, Decoux V, Leban J-M. 2006. Linking intra-tree-ring wood density variations and tracheid anatomical characteristics in Douglas fir (*Pseudotsuga menziesii* (Mirb.) Franco). *Annals of Forest Science* **63**: 699-706.

Rathgeber C, Misson L, Nicault A, Guiot J. 2005. Bioclimatic model of tree radial growth: application to the French Mediterranean Aleppo pine forests. *Trees* **19**: 162-176.

Rossi S, Morin H, Deslauriers A. 2012. Causes and correlations in cambium phenology: towards an integrated framework of xylogenesis. *J Exp Bot* **63**(5): 2117-2126.

Sass-Klaassen U, Fonti P, Cherubini P, Gricar J, Robert EM, Steppe K, Brauning A. 2016. A Tree-Centered Approach to Assess Impacts of Extreme Climatic Events on Forests. *Front Plant Sci* **7**: 1069.

Schweingruber FH, Fritts HC, Bräker OU, Drew LG, Schär E. 1978. The X-ray technique as applied to dendroclimatology. *Tree-Ring Bulletin* **38**: 61-91.

Seo JW, Eckstein D, Jalkanen R, Rickebusch S, Schmitt U. 2008. Estimating the onset of cambial activity in Scots pine in northern Finland by means of the heat-sum approach. *Tree Physiology* **28**(1): 105-112.

Sperry JS, Hacke UG, J P. 2006. Size and function in conifer tracheids and angiosperm vessels. *American Journal of Botany* **93**(10): 1490-1500.

Sperry J S, Nichols K L, June E M S, Eastlack S E. 1994. Xylem Embolism in Ring- Porous, Diffuse-Porous, and Coniferous Trees of Northern Utah and Interior Alaska. *Ecology* **75,** 1736-1752.

St. George S. 2014. An overview of tree-ring width records across the Northern Hemisphere. *Quaternary Science Reviews* **95**: 132-150.

Stoffel M, Khodri M, Corona C, Guillet S, Poulain V, Bekki S, Guiot J, Luckman BH, Oppenheimer C, Lebas N, et al. 2015. Estimates of volcanic-induced cooling in the Northern Hemisphere over the past 1,500 years. *Nature Geoscience* **8**(10): 784-788.

Tibshirani R, Walther G, Hastie T. 2001. Estimating the number of clusters in a data set via the gap statistic. *Journal of the Royal Statistical Society: Series B* **63**(2): 411-423.

Trenberth KE, Shea DJ. 2005. Relationships between precipitation and surface temperature. *Geophysical Research Letters* **32**(14) 1-4.

Tyree MT, Ewers FW. 1991. The hydraulic architecture of trees and other woody plants. *New Phytol* **119**(3): 345-360.

Tyree MT, Zimmermann MH 2002. Xylem Structure and the Ascent of Sap. Berlin, Germany: Springer.

Vaganov EA, Hughes MK, Shashkin AV. 2006. *Growth Dynamics of Conifer Tree Rings: Images of Past and Future Environments*: Springer Berlin Heidelberg.

Vaganov E A, Schulze E-D, Skomarkova M V, Knohl A, Brand W A, Roscher C. 2009. Intra-annual variability of anatomical structure and δC values within tree rings of spruce and pine in alpine, temperate and boreal Europe. *Oecologia* **161**: 729-745.

Wang L, Payette S, Bégin Y. 2002. Relationships between anatomical and densitometric characteristics of black spruce and summer temperature at tree line in northern Quebec. *Canadian Journal of Forest Research* **32**(3): 477-486.

Wigley TM, Briffa KR, Jones PD. 1984. On the average value of correlated time series, with applications in dendroclimatology and hydrometeorology. *Journal of climate and Applied Meteorology* **23**(2): 201-213.

Wilson R, Anchukaitis K, Briffa KR, Büntgen U, Cook E, D'Arrigo R, Davi N, Esper J, Frank D, Gunnarson B, et al. 2016. Last millennium northern hemisphere summer temperatures from tree rings: Part I: The long term context. *Quaternary Science Reviews* **134**: 1-18.

Wodzicki TJ. 1971. Mechanism of Xylem Differentiation in Pinus silvestris L. *Journal of Experimental Botany* **22**(3): 670-687.

The following Supporting Information is available for this article:

Tab. S1 Top 10 most common species in the Northern Hemisphere densitometric network.
Fig. S1 X-ray images for ten of the most abundant species in the network
Fig. S2 Map of lengths of chronologies in the NH Network.
Fig. S3 *Rbar* statistic for each chronology and parameter in the NH-network
Fig. S4 Examples how to calculate bivariate univariate density parameters
Fig. S5 Correlation coefficients between different pairs of ring widths, and densities
Fig. S6 Hovmöller diagrams over precipitation correlations of NH-network data
Fig. S7 Complete results of the cluster identification of the NH-network data.
Fig. S8 Standard deviations and averages of different anatomical parameters,
Fig. S9 Correlation coefficients between different anatomical parameters
Notes S1 NH-network quality screening
Notes S2 NH-network overview
Notes S3 Rbar, the strength of the common signal in the NH-network
Notes S4 Cell anatomical data details
Notes S5 List of abbreviations